3D FREEHAND ULTRASOUND RECONSTRUCTION AND CROSS-WIRE CALIBRATION

Ing. Asterios ANAGNOSTOUDIS, Doctoral Degree Programme (2)
Dept. of Biomedical Engineering, FEEC, BUT
E-mail: asterios@feec.vutbr.cz

Supervised by: Prof. Jiří Jan

ABSTRACT

3D freehand ultrasound is an imaging technique, which is rapidly finding clinical applications. A position sensor is attached to a conventional ultrasound probe, so that B-scans are acquired along with their relative locations. This allows the B-scans to be inserted into a 3D regular voxel array, which can then be visualised using arbitrary-plane slicing, and volume and surface rendering. A key requirement for reconstruction is calibration: determining the position and orientation of the B-scans with respect to the position sensor's receiver. Following calibration, interpolation of the set of irregularly spaced B-scans is required to reconstruct a regular voxel array. This text describes a freehand measurement of 2D ultrasound data and an approach to their 3D reconstruction.

1 INTRODUCTION

Conventional 2D ultrasound imaging uses a hand-held probe, which transmits ultrasound pulses into the body and receives the echoes. The magnitude and the timing of the echoes are used to create a 2D grey-level image (B-scan) of a cross-section of the body in the scan plane. 3D ultrasound extends this concept so that volumes of intensity data are created from pulse-echo information.

The 3D freehand imaging technique can be broken into three stages: scanning, reconstruction, and visualisation. We move freely a conventional ultrasound probe over the patient's body, so that the acquired B-scans can have arbitrary relative locations and may overlap with other. A position sensor, consisting of an electromagnetic receiver and transmitter, is used to determine the position and orientation of the acquired B-scans. Before scanning, the receiver is attached to the probe and the transmitter is placed in a fixed position. In the next stage, the set of acquired B-scans and their relative positions are used to fill a regular voxel array, which can then be visualized using arbitrary-plane slicing [5], volume [6] and surface rendering [7].

2 RECONSTRUCTION

The measurement has been done with the Vingmed Five system (GE Vingmed ultrasound) with a linear 2.5 MHz FPA probe. The position sensor was the electromagnetic miniBIRD system (Ascension). Figure 1 shows the four coordinate systems used for reconstruction. **P** is the coordinate system of the B-scan plane. In [1] the coordinate system of P is placed at the top left corner of a cropped B-scan. In our example, we place it in the vertex of the original B-scan, which corresponds to the centre of the front (radiating) side of the probe. The y-axis is in the beam direction, the x-axis is in the lateral direction and the z-axis in the elevation direction, out of the plane of the B-scan. **R** is the coordinate system of the moving receiver and **T** is the coordinate system of the fixed transmitter. The reconstruction volume, created from the set of acquired B-scans, takes the form of a 3D matrix of volume elements (voxels). **C** is the coordinate system of the volume, placed at its corner.

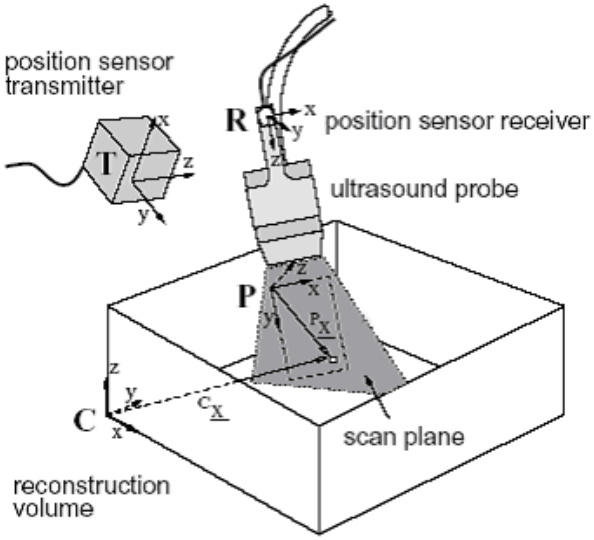

Fig. 1: The four coordinate systems used during the reconstruction process

During reconstruction, every pixel in every B-scan has to be located with respect to the reconstruction volume. Each pixel's scan plane location, represented by the vector ${}^{P}\underline{x}$, is transformed to the coordinate system of the receiver R, then to the transmitter T and finally to the reconstruction volume C. The overall transformation can be expressed as the multiplication of homogeneous transformation matrices [1, 2]:

$$ {}^{C}\underline{x} = {}^{C}T_{T} \cdot {}^{T}T_{R} \cdot {}^{R}T_{P} \cdot {}^{P}\underline{x}, \qquad \text{where } {}^{P}\underline{x} = \begin{pmatrix} s_x \cdot u & s_y \cdot v & 0 & 1 \end{pmatrix}^{T} \tag{1} $$

${}^{C}\underline{x}$ is a vector representing the pixel's location in the coordinate system C, ${}^{J}T_{I}$ is the transformation from the coordinate system I to the coordinate system J, u and v are the column and row indices of the pixel in the B-scan, and s_x and s_y are scale factors [mm/pixel].

A transformation between two coordinate systems has six degrees of freedom: three rotations (α, β, γ) and three translations (x, y, z). The rotation between two coordinate systems is effected by first rotating through α around the x-axis (elevation), then through β around the y-axis (azimuth), and finally through γ around the z-axis (roll). The fixed rotation axes are aligned with the first coordinate system. Using this convention, the homogeneous matrix describing the transformation takes the following form:

$$
{}^{J}T_{I}(x,z,y,\alpha,\beta,\gamma) =
\begin{pmatrix}
\cos\alpha\cdot\cos\beta & \cos\alpha\cdot\sin\beta\cdot\sin\gamma-\sin\alpha\cdot\cos\gamma & \cos\alpha\cdot\sin\beta\cdot\cos\gamma+\sin\alpha\cdot\sin\gamma & x \\
\sin\alpha\cdot\cos\beta & \sin\alpha\cdot\sin\beta\cdot\sin\gamma+\cos\alpha\cdot\cos\gamma & \sin\alpha\cdot\sin\beta\cdot\cos\gamma-\cos\alpha\cdot\sin\gamma & y \\
-\sin\beta & \cos\beta\cdot\sin\gamma & \cos\beta\cdot\cos\gamma & z \\
0 & 0 & 0 & 1
\end{pmatrix} \quad (2)
$$

The transformation matrix ${}^{T}T_{R}$, giving the position and orientation of the moving receiver with respect to the fixed transmitter, is derived directly from the position sensor readings. To simplify the computations, we could omit ${}^{C}T_{T}$ and align the reconstruction volume with the transmitter, but this might for instance, place the B-scans away from the origin of C, resulting in a largely empty voxel array. Or the anatomy might appear upside down, with the head towards the bottom of the reconstructed volume and the feet towards the top: it all depends on the positioning of the transmitter with respect to the patient. That leaves just ${}^{R}T_{P}$ and the scale factors s_x and s_y, which need to be determined by calibration.

3 CALIBRATION

Calibration [1, 2] is performed by scanning a phantom of known geometric dimensions. Equations similar to (1) can be written using knowledge of the phantom geometry and the position sensor measurements. These equations are then solved to determine the calibration parameters. In our measurement, we used the common cross-wire calibration phantom. Two intersecting wires of 0.3 mm diameter are mounted in a water bath with the transmitter placed at some fixed location with respect to the wires (under the patient's bed). For calibration purposes, the origin of C is not coincident with the corner of the reconstruction volume, but is placed instead at the intersection of the wires [1]. This simplifies the calibration equations. The location where the wires cross is scanned repeatedly from different directions, with each B-scan showing a detectable cross. The B-scan pixel at the centre of the cross should satisfy:

$$
\begin{pmatrix} 0 \\ 0 \\ 0 \\ 1 \end{pmatrix} = {}^{C}T_{T}\cdot{}^{T}T_{R}\cdot{}^{R}T_{P}\cdot\begin{pmatrix} s_x\cdot u \\ s_y\cdot v \\ 0 \\ 1 \end{pmatrix} \quad (3)
$$

The first three rows of (3) give three equations involving the measurements ${}^{T}T_{R}$, u and v, and the unknowns ${}^{R}T_{P}$, ${}^{C}T_{T}$, s_x and s_y. If there are m B-scans, then the equations can be stacked together to produce a system of non-linear homogeneous equations of size 3m (we have measured 30 B-scans):

$$
0 = f(\theta,\phi) \quad (4)
$$

where θ are the measurements ${}^{T}T_{R}$, u and v and ϕ are the unknowns ${}^{R}T_{P}$, ${}^{C}T_{T}$, s_x and s_y. The system can be solved by several iterative methods, such us the Levenberg-Marquardt algorithm used in [1].

For calibration, we are only interested in ${}^{R}T_{P}$, but we must also solve for ${}^{C}T_{T}$, even

though we will subsequently discard these values and adopt an arbitrary, convenient ${}^{C}T_{T}$ for reconstruction as explained previously. The scale factors are regarded as unknowns and included in ϕ for more accurate and automatic estimates. The row and column indices (u, v) of the cross-wire intersection point can be detected either manually or automatically by a feature detection algorithm. Since the detectable point in the B-scan covers an area of pixels, we can consider the middle pixel of the area as the one corresponding to the calibration point. Therefore, it appears that ϕ must be a 14-element vector, composed of the 6 parameters of ${}^{R}T_{P}$, the 6 parameters of ${}^{C}T_{T}$ and the 2 scale factors. However, it is clear from inspection of the geometry that the coordinate system C can be at any orientation and still satisfy (3). This means that the three orientation angles of ${}^{C}T_{T}$ can be removed from ϕ and for convenience set to zero in (4). This simplifies the calculations further making ϕ an 11-element vector. The position x, y, z of the volume's coordinate system can be chosen as required for each examination.

4 INTERPOLATION

Following calibration and therefore localization of each B-scan in space, the interpolation of the set of irregularly spaced B-scans is required to reconstruct a regular voxel array. Some of the several interpolation techniques used for this purpose are described here.

During voxel nearest neighbor interpolation (VNN) [3, 4], each voxel is assigned the value of the nearest pixel. There are no parameters to set. A naive implementation would traverse the array one voxel at a time and find the nearest pixel, but this would be computationally inefficient. Using the fact that the nearest pixel lies on a line normal to the nearest B-scan greatly speeds up the reconstruction, making it one of the fastest of all methods. This reconstruction method has the advantage of avoiding gaps in the voxel array, but reconstruction artefacts can be observed in slices through the voxel array. When a slice plane intersects several of the original B-scans, we can consider the interpolated image as a collage of projections from the intersected B-scans. Registration errors, including tissue motion and sensor errors, contribute to slight misalignment of the B-scans. This results in a piece of the collage slightly mismatching its neighbours. The lines of intersection between the pieces then become visible.

Pixel nearest neighbor interpolation (PNN) [3, 4], is one of the most popular reconstruction methods. The basic algorithm consists of two stages. In the first stage (bin filling), the algorithm simply runs through each pixel in every B-scan and fills the nearest voxel with the value of that pixel. Multiple contributions to the same voxel are usually averaged. The parameters to set at this stage are therefore the weights on the multiple contributions. If the voxel size is small compared to the distance between the acquired B-scans, gaps can occur in the voxel array. The second stage (hole filling) fills these remaining gaps in the voxel array. A variety of methods, have been used, including averaging of filled voxels in a local neighbourhood and interpolating between the two closest non-empty voxels. Alternatively, we can choose the voxel size sufficiently large to avoid gaps. The parameters to set at this stage are the weights of the nearby voxels used to fill the gaps. Unfortunately, artefacts can be generated by this two-stage process. For example, a slice plane passing though regions of both first stage and second stage filled voxels may show the boundary between the highly detailed „bin-filled“ voxels and the smoothed „hole-filled“ voxels.

Like the voxel nearest neighbour interpolation method, distance-weighted (DW)

interpolation [3, 4] proceeds voxel by voxel but assigns a value to each voxel based on a weighed average of some set of pixels from nearby B-scans. The parameters to choose are the weight function and the size and shape of the neighbourhood. The simplest approach is to consider a fixed spherical neighbourhood of radius R, centred about each voxel. All pixels in this neighbourhood are weighted by the inverse distance to the voxel and then averaged. If R is set too small, gaps may result. Yet if R is set too large, the voxel array will appear highly smoothed, since the effect of inverse distance weighting can be quickly overwhelmed by the much larger number of data points falling into the larger local neighbourhood. Nevertheless, with dense B-cans and a small value of R, excellent results are claimed.

5 CONCLUSIONS

We have presented an approach to 3D freehand ultrasound reconstruction using an electromagnetic position sensor for localisation of the receiver with respect to a fixed transmitter and the common cross-wire calibration phantom for the localisation of the B-scan's with respect to the receiver. The calibration measurement is time consuming but reconstruction with such a type of calibration claims good results. Other types of calibration include: three-wire [1] and wall calibration [1, 2]

ACKNOWLEDGEMENTS

The paper is a partial result of the project supported by the grant No. 102/02/0890 of the grant agency of the Czech Republic and partly also by the grant CEZ J22/98: 262200011 of the Ministry of education of the Czech Republic.

REFERENCES

[1] Prager, R. W., Rohling, R. N., Gee, A. H., and Berman, L. Automatic calibration for 3D freehand ultrasound. Technical Report CUED/F-INFENG/TR303, Cambridge University Engineering Department, 1997.

[2] Rousseau, F., Hellier, P., and Barillot, C. Robust and automatic calibration method for 3D freehand ultrasound. In Medical Image Computing and Computer Assisted Intervention, MICCAI'03, Montreal, Canada, November 2003.

[3] Rohling, R. N., Gee, A. H., and Berman, L. A comparison of freehand 3D ultrasound reconstruction techniques. Medical Image Analysis, 1999, 3(4): 339-359.

[4] Rohling, R. N., Gee, A. H., and Berman, L. Spatial compounding of 3D ultrasound images. Medical Image Analysis, 1997, 1(3): 177-193.

[5] Prager, R. W., Gee, A. H., and Berman, L. Stradx: Real time acquisition and visualisation of freehand 3D ultrasound. Medical Image Analysis, 1999, 3(2): 129-140.

[6] Prager, R. W., Treece, G. M., and Berman, L. Narrow-band volume rendering for freehand 3D ultrasound. Computer And Graphics, 2002, 26: 463-476.

[7] Treece, G. M., Prager, R. W., Gee, A. H., and Berman, L. Fast surface and volume estimation from non-parallel cross-sections for freehand 3D ultrasound. Medical Image Analysis, 1999, 3(2): 141:173.